ACTA ONCOLOGICA, 2017
VOL. 56, NO. 3, 490–498
http://dx.doi.org/10.1080/0284186X.2016.1273544

Taylor & Francis
Taylor & Francis Group

LETTER TO THE EDITOR

Knowledge-based planning for stereotactic radiotherapy of peripheral early-stage lung cancer

Alexander R. Delaney, Max Dahele, Jim P. Tol, Ben J. Slotman and Wilko F. A. R. Verbakel

Department of Radiotherapy, VU University Medical Center, Amsterdam, The Netherlands

Peripheral early-stage non-small cell lung cancer in medically inoperable patients is a guideline-recommended indication for stereotactic body radiotherapy (SBRT) [1]. However, peripheral lesions present varying tumor geometries and overlap with organs at risk (OARs) such as the thoracic wall (TW); treatment planning is prone to variation, leading to inconsistencies in treatment plan (TP) quality [2,3]; and implementing a lung SBRT program is resource intensive [4]. Automated solutions have been devised to help address these problems, including knowledge-based planning (KBP) [5–10].

One commercial KBP solution utilizes a model based on previous TPs to generate dose-volume histogram (DVH) prediction ranges which position optimization objectives for the OARs of prospective patients. Pre-clinical evaluation has yielded clinically acceptable results for a number of disease sites [11–13]. However, detailed investigations for lung SBRT are lacking. We therefore investigated the performance of this KBP solution for 3 and 5 fraction lung SBRT using volumetric modulated arc therapy (VMAT); whether TPs from these fractionation schemes could be combined into a single model; and how the models performed when the planning target volume (PTV) overlapped with OARs including the TW.

Material and methods

Lung SBRT is treated using flattening filter-free beams and VMAT [14]. Risk-adapted fractionation schemes are applied, for example 3×18 Gy for peripheral tumors <3 cm in diameter, without broad TW contact and 5×11 Gy for tumors >3 cm or with broad TW contact. Both schemes allow inhomogeneous PTV doses up to 140% of the prescribed dose. When there is PTV-TW overlap, two target structures, PTVinOAR/PTVoutOAR, are created for the part of the PTV with/without TW overlap. Maximum dose (D_{max}) is restricted to $\leq$140% of the prescribed dose in PTVoutOAR and $\leq$110% in PTVinOAR. A 1–2 cm wide TW structure is delineated to control TW dose outside the PTV. Optimization objectives limit the volume receiving 30–60 Gy ($V_{30\text{-}60}$), which may be predictive for TW toxicity [15]. A 5-mm wide ring structure 5 mm from the PTV, and a normal tissue objective (NTO), are used for dose fall off. To limit irradiation of the contralateral lung, a dose objective on the V_5 [16] as well as a partial arc/avoidance sector are used. A maximum dose objective is used for the spinal cord, and a 3-mm planning-at-risk volume (Table S1). Finally, all TPs undergo a continue previous optimization (CPO) [17,18], as described in Appendix 1 of the supplementary materials.

RapidPlan™ is a commercial KBP solution constituting a model derived from a library of TPs. Models use regression analysis to determine correlations between dosimetric and geometric features, with the coefficient of determination (R^2) indicative of the quality and variance of regression models [13]. The model generates DVH prediction ranges for OARs of prospective patients. Optimization objectives are then placed along the lower boundary of these prediction ranges to guide the VMAT optimization [12].

Clinical plans (CPs) of 100 patients were used to populate three models: $Model_{5 \times 11}$/$Model_{3 \times 18}$ comprised CPs of 50 patients treated with 5×11 Gy/3×18 Gy; $Model_{COMBI}$ comprised all 100 plans, and is therefore more heterogeneous in terms of dosimetry, fractionation, arc configuration, and geometry (Table S2).

An evaluation group (EG) comprised 20 further CPs (10 each of 5×11 Gy/3×18 Gy). CPs were optimized using PRO v10.0.28 (PRO10) and dose was calculated using AcurosXB v11.0.31. Two KBPs were created for each evaluation patient using the Photon Optimizer v13.6.15 (PO13). The first used $Model_{3 \times 18}$ or $Model_{5 \times 11}$ depending on the CP fractionation; the second used $Model_{COMBI}$. Both used the CP arc setup. To limit user interaction, KBPs utilized DVH predictions for all of the OAR objectives, except for the dose-volume objective limiting the contralateral lung V_5 (Table S3), and an automatic NTO. Dose was calculated using AcurosXB v13.6.15 with a 2.5 mm calculation grid. Both CPs and KBPs were normalized such that 95% of the PTV received the prescribed dose. To account for differences between optimizers, all CPs in the EG were re-optimized using PO13 (CP_{PO}), using the same arc configuration, end-clinical objectives, and priorities.

Model quality was evaluated using statistical metrics/regression plots reported by RapidPlan and Model Analytics (https://modelanalytics.varian.com), facilitating outlier identification [19]. Furthermore, KBPs generated by $Model_{3 \times 18/5 \times 11}$ and $Model_{COMBI}$ were compared with their respective CPs

CONTACT Alexander R. Delaney a.delaney@vumc.nl Department of Radiotherapy, VU University Medical Center, De Boelelaan 1117, 1081 HV Amsterdam, The Netherlands

Supplemental data for this article can be accessed here.

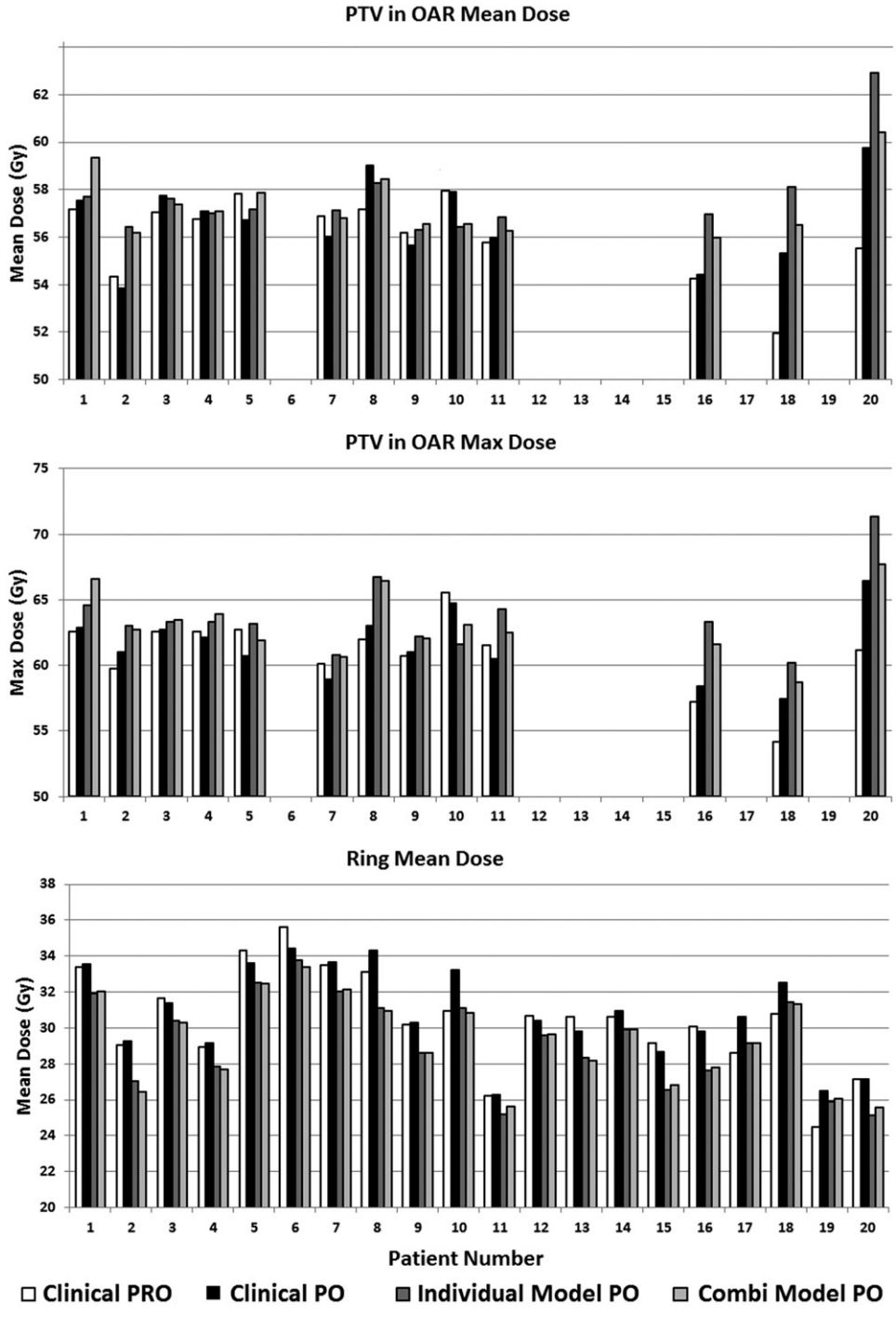

Figure 1. Dosimetric results per patient. Patients 1–10 are 5×11 Gy cases while 11–20 are 3×18 Gy.

using OAR and PTV dose metrics. Where appropriate two-sided Student's t-tests, or for skewed data the Kruskal-Wallis test, were performed with $p < 0.05$ considered significant.

Results

$Model_{3 \times 18}$, $Model_{5 \times 11}$ and $Model_{COMBI}$ had 34, 19 and 73 structures identified as outliers, respectively, by at least one model metric. Of these, 2/34, 0/19 and 4/73 were visually confirmed and removed [19]. Two PTVinOAR structures with the smallest volumes ($0.2\,cm^3$) were removed as their respective DVHs were insufficiently sampled during the extraction phase of model creation [13] leading to inaccurate DVH representation in the model configuration window. Regression analysis of models showed good correlation between geometric and dosimetric features; average R^2 was 0.75, 0.80 and 0.76 for $Model_{3 \times 18}$, $Model_{5 \times 11}$ and $Model_{COMBI}$, respectively (Figure S1). R^2 for the TW and contralateral lung in $Model_{3 \times 18}$/$Model_{5 \times 11}$/$Model_{COMBI}$ was

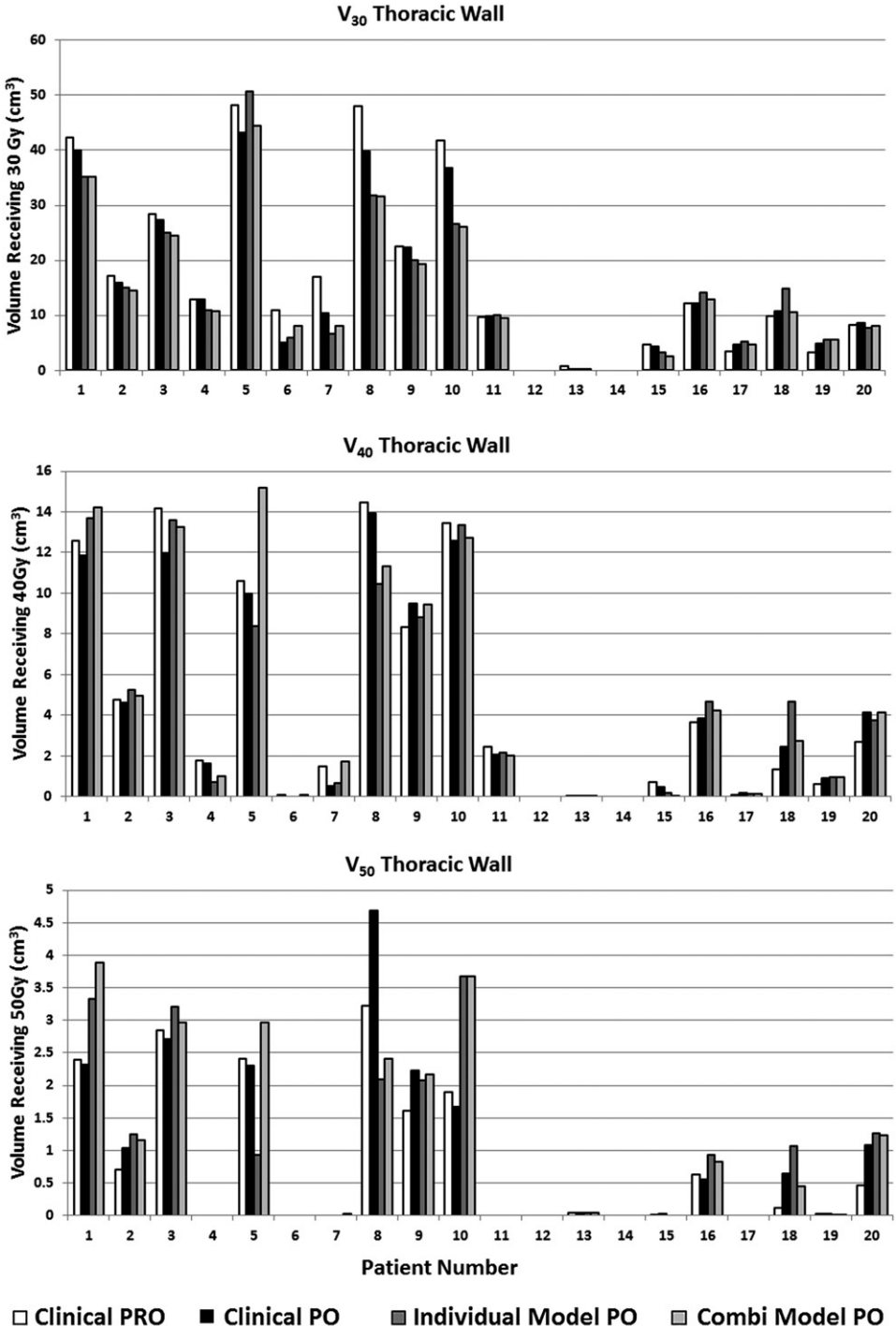

Figure 2. Dosimetric results per patient.

0.88/0.88/0.91 and 0.74/0.81/0.73, respectively. Figure S1 shows the majority of 5×11 Gy and 3×18 Gy patients are located in different regions of the regression plot consistent with differences in their TW dosimetry/geometry. The ring structure had the lowest R^2: 0.59/0.59/0.60 in $Model_{3 \times 18}$/ $Model_{5 \times 11}$/$Model_{COMBI}$.

Figures 1 and 2 compare individual results for all 20 patients from CP, CP_{PO}, $Model_{3 \times 18/5 \times 11}$ and $Model_{COMBI}$, while Tables 1 and 2 summarize averaged results. Re-optimization of CPs using PO13 led to similar plan quality, however differences existed in certain patients, mainly for the PTVinOAR, TW V_{50} and ring. Using $Model_{COMBI}$ produced, on average, similar plan quality to the respective individual $Model_{3 \times 18/5 \times 11}$.

KBPs of nine patients exhibited increases in both D_{mean} and D_{max} to the PTVinOAR over CP_{PO} (Figure 1). This was associated with a decrease in ring D_{mean}. For some of these patients, the differences were more pronounced when compared to the CP. In 8/9 cases the KBP PTVinOAR D_{mean} was $\leq$110% of the prescribed dose and following review by a physician and

Table 1. Averaged RapidPlan results for 5×11 Gy patients of EG using $Model_{5 \times 11}$ and $Model_{COMBI}$ compared with respective clinical plans and clinical plans re-optimized using P013 [Clinical(PO)].

	Evaluation group (EG)			
	5×11 Gy patients			
	Clinical	Clinical (PO)	$Model_{5 \times 11}$	$Model_{COMBI}$
Volume receiving × Gy (%)				
C. lung V_5	0.8 ± 1.1	1.2 ± 1.3	1.6 ± 2.0	1.6 ± 1.9
Total lung – PTV V_5	12.7 ± 3.3	12.8 ± 3.2	12.6 ± 3.2	12.5 ± 3.2
Total lung – PTV V_{20} (cm^3)	4.0 ± 2.0	4.1 ± 2.0	3.8 ± 1.9	3.8 ± 1.9
Thoracic wall V_{30}	28.9 ± 14.9	25.4 ± 14.0[c]	22.8 ± 14.1[c]	22.3 ± 12.3[a,c]
Thoracic wall V_{40}	8.2 ± 5.7	7.7 ± 5.4	7.5 ± 5.5	8.4 ± 5.9
Thoracic wall V_{50}	1.5 ± 1.2	1.7 ± 1.5	1.7 ± 1.4	1.9 ± 1.5
Mean dose (Gy)				
ITV	67.6 ± 1.9	66.6 ± 2.2	67.7 ± 2.9	67.5 ± 2.4
PTV out OAR	63.6 ± 1.4	63.0 ± 1.8	63.5 ± 1.2	63.4 ± 0.9
PTV in OAR	56.8 ± 1.1	56.8 ± 1.5	57.1 ± 0.7	57.4 ± 1.0
C. lung	0.8 ± 0.3	0.9 ± 0.3	0.9 ± 0.3	0.9 ± 0.3
Total lung – PTV	2.9 ± 0.9	2.9 ± 0.9	2.8 ± 0.9[c]	2.8 ± 0.8[c]
Ring	32.1 ± 2.3	32.3 ± 2.1	30.6 ± 2.2	30.5 ± 2.3
Max dose (Gy)				
PTV in OAR	62.1 ± 1.7	61.9 ± 1.7	63.2 ± 1.7	63.4 ± 2.0[a]
Thoracic wall	54.7 ± 7.0	55.6 ± 7.9	54.3 ± 8.7	56.3 ± 7.3[b]
Spinal cord	8.0 ± 4.3	8.2 ± 4.0	7.6 ± 2.2	8.3 ± 3.5
Esophagus	8.3 ± 4.0	9.4 ± 4.2[c]	10.6 ± 5.1[c]	10.7 ± 5.0[c]
Trachea	6.8 ± 6.4	8.1 ± 6.9[c]	8.6 ± 7.1	8.0 ± 6.5
Monitor units	2898 ± 497	2754 ± 335	2976 ± 452	2942 ± 452

C. lung: Contralateral lung; V_X: volume receiving × Gy.
[a]Indicates a statistically significant difference ($p < 0.05$) between $Model_{5 \times 11/COMBI}$ and Clinical(PO);
[b]Indicates a statistically significant difference ($p < 0.05$) between $Model_{COMBI}$ and $Model_{5 \times 11}$;
[c]Indicates a statistically significant difference ($p < 0.05$) between Clinical and Clinical(PO) or $Model_{5 \times 11/COMBI}$.

Table 2. Averaged RapidPlan results for 3×18 Gy patients of EG using $Model_{3 \times 18}$ and $Model_{COMBI}$ compared with respective clinical plans and clinical plans re-optimized using P013 [Clinical(PO)].

	Evaluation group (EG)			
	3×18 Gy patients			
	Clinical	Clinical (PO)	$Model_{3 \times 18}$	$Model_{COMBI}$
Volume receiving × Gy (%)				
C. lung V_5	0.1 ± 0.2	0.3 ± 0.4	0.1 ± 0.2	0.3 ± 0.3
Total lung – PTV V_5	11.0 ± 3.1	11.0 ± 3.1	10.7 ± 3.2[a]	10.7 ± 3.3
Total lung – PTV V_{20} (cm^3)	2.3 ± 1.2	2.3 ± 1.1	2.0 ± 1.0[a,c]	2.0 ± 1.0[a,b,c]
Thoracic wall V_{30}	5.8 ± 4.3	6.1 ± 4.5	6.8 ± 5.5	6.0 ± 4.6
Thoracic wall V_{40}	1.3 ± 1.3	1.6 ± 1.6	1.8 ± 2.0	1.6 ± 1.8
Thoracic wall V_{50}	0.1 ± 0.2	0.3 ± 0.4	0.4 ± 0.5	0.3 ± 0.5
Mean dose (Gy)				
ITV	67.2 ± 3.0	66.7 ± 3.0	69.9 ± 3.3[a,c]	69.3 ± 3.5[a,b,c]
PTV out OAR	61.8 ± 1.2	61.3 ± 1.2	62.9 ± 1.3[a,c]	62.7 ± 1.3[a]
PTV in OAR	54.4 ± 1.8	56.4 ± 2.4	58.7 ± 2.9[a]	57.3 ± 2.1[c]
C. lung	0.5 ± 0.2	0.5 ± 0.2	0.5 ± 0.1	0.5 ± 0.1
Total lung – PTV	2.1 ± 0.6	2.1 ± 0.6	2.0 ± 0.6	2.0 ± 0.6
Ring	28.8 ± 2.2	29.3 ± 2.1	27.9 ± 2.2[a]	28.0 ± 2.0[a]
Max dose (Gy)				
PTV in OAR	58.5 ± 3.5	60.7 ± 4.0	64.8 ± 4.7[a,c]	62.6 ± 3.7[a,b,c]
Thoracic wall	51.1 ± 9.3	53.0 ± 11.1	54.1 ± 12.5	52.5 ± 11.4
Spinal cord	4.7 ± 4.4	4.8 ± 3.5	3.7 ± 1.0	4.5 ± 2.8
Esophagus	6.3 ± 2.4	6.4 ± 2.6	7.1 ± 2.8[a,c]	7.1 ± 2.3[a]
Trachea	4.0 ± 2.8	4.7 ± 3.1[c]	5.8 ± 4.2[c]	5.3 ± 3.5[c]
Monitor units	6507 ± 1346	4653 ± 477[c]	5037 ± 501[a,c]	4895 ± 499[b,c]

C. lung: contralateral lung; V_X: volume receiving × Gy.
[a]Indicates a statistically significant difference ($p < 0.05$) between $Model_{3 \times 18/COMBI}$ and Clinical(PO);
[b]Indicates a statistically significant difference ($p < 0.05$) between $Model_{COMBI}$ and $Model_{3 \times 18}$;
[c]Indicates a statistically significant difference ($p < 0.05$) between Clinical and Clinical(PO) or $Model_{3 \times 18/COMBI}$.

physicist, these plans were considered clinically acceptable. For the remaining patient (20), CP_{PO} showed a relatively large increase in PTVinOAR $D_{mean/max}$ when compared to CP, (PRO10). The dose increased further when using $Model_{3\times18}$, while $Model_{COMBI}$ performed similarly to CP_{PO}. The KBP ring D_{mean} for this patient was the lowest among evaluation cases.

Discussion

We evaluated a commercial KBP solution for risk-adapted peripheral lung SBRT VMAT treatment planning. On average, two dose-fractionation-specific models generated plans of comparable quality to their respective clinical plan. Additionally, a larger, combined model, could be successfully created using plans with different fractionation and arc setup (partial arcs or avoidance sectors), but with similar total dose and planning goals. In some cases, the combined model led to dosimetric improvements compared to the fraction-specific model, likely because of increased geometric heterogeneity. In total, 39/40 KBPs (98%) would have been considered clinically acceptable (one plan, for Patient 20, would have been rejected due to a high PTVinOAR $D_{mean/max}$ with $Model_{3\times18}$).

Regression plots (Figure S1) and R^2 values suggest models generally provided good correlation between dosimetric and geometric features. However, the ring was modeled less well with the lowest R^2 amongst the OARs, and ring D_{mean} decreased for all patients when using KBPs over CP_{PO}. Reasons for this are still uncertain. We currently use a ring structure and NTO with standard settings. NTO modifications, for example with model-predicted settings based on PTV geometry, might remove the necessity for a ring structure.

PTVinOAR dose increased in a number of cases, particularly for those with a small volume (PTVinOAR for Patients 2, 16, 18 and 20 was $<0.7\,cm^3$). Several contributing factors were identified. First, the model does not predict PTVinOAR doses, as it is not an OAR. Furthermore, when the ring structure extends into the TW and the ring prediction is too low compared to the TW (Patient 20), TW sparing is compromised resulting in higher PTVinOAR doses. Second, model composition may have been an issue with only nine patients with chest wall overlapping/touching the PTV in $Model_{3\times18}$. Finally, some cases exhibited large differences between CP and CP_{PO} plans. The CPO is needed to correct dose in low density regions resulting from the initial optimization, which attributes more dose to higher density regions (e.g. PTVinOAR). However, we found that the CPO in PO13 stopped prematurely and that PO13 seemed to inherently minimize MUs to a greater extent than PRO10 (Appendix 2 of the supplementary materials). This has been communicated to the manufacturer. Early evaluation of a preliminary solution provided by the manufacturer appeared to resolve this issue although this is not yet clinically available.

In conclusion, KBPs were, on average, of comparable quality to their respective CPs for 3 and 5 fraction peripheral lung SBRT treatments, however, differences were noted for individual patients. All plans therefore needed to be critically reviewed. Plan quality generated by $Model_{COMBI}$ showed that TPs with differing fractionation schemes, but similar total prescription doses and planning strategies, could be used to populate a combined model. Deviations from CPs seemed to be largely attributable to the inherent mechanics of the PO13 optimizer, which are different to PRO10. This requires further investigation by the manufacturer. Finally, caution should be exercised when dealing with structures poorly represented in a knowledge-based model.

Disclosure statement

The department has a research collaboration with Varian Medical Systems, and Dahele, Slotman, and Verbakel have received honoraria/travel support from Varian Medical Systems.

Funding

This research was supported by a grant from Varian Medical Systems.

References

[1] Lagerwaard FJ, Haasbeek CJA, Smit EF, et al. Outcomes of risk-adapted fractionated stereotactic radiotherapy for stage I non-small-cell lung cancer. Int J Radiat Oncol Biol Phys. 2008;70:685–692.
[2] Nelms BE, Robinson G, Markham J, et al. Variation in external beam treatment plan quality: an inter-institutional study of planners and planning systems. Pract Radiat Oncol. 2012;2:296–305.
[3] Das IJ, Cheng CW, Chopra KL, et al. Intensity-modulated radiation therapy dose prescription, recording, and delivery: patterns of variability among institutions and treatment planning systems. J Natl Cancer Inst. 2008;100:300–307.
[4] Khader J, Al-Mousa A, Hijla FA, et al. Requirements and implementation of a lung sbrt program in a developing country: benefits of international cooperation. Int J Radiat Oncol Biol Phys. 2016;95:1236–1238.
[5] Wu B, Pang D, Simari P, et al. Using overlap volume histogram and IMRT plan data to guide and automate VMAT planning: a head-and-neck case study. Med Phys. 2013;40:021714.
[6] Lian J, Yuan L, Ge Y, et al. Modeling the dosimetry of organ-at-risk in head and neck IMRT planning: an intertechnique and inter-institutional study. Med Phys. 2013;40:121704.
[7] Zhu X, Ge Y, Li T, et al. A planning quality evaluation tool for prostate adaptive IMRT based on machine learning. Med Phys. 2011;38:719.
[8] Moore KL, Brame RS, Low DA, et al. Experience-based quality control of clinical intensity-modulated radiotherapy planning. Int J Radiat Oncol Biol Phys. 2011;81:545–551.
[9] Zarepisheh M, Long T, Li N, et al. A DVH-guided IMRT optimization algorithm for automatic treatment planning and adaptive radiotherapy replanning. Med Phys. 2014;41:061711.
[10] Good D, Lo J, Lee WR, et al. A knowledge-based approach to improving and homogenizing intensity modulated radiation therapy planning quality among treatment centers: an example application to prostate cancer planning. Int J Radiat Oncol Biol Phys. 2013;87:176–181.
[11] Fogliata A, Nicolini G, Clivio A, et al. A broad scope knowledge based model for optimization of VMAT in esophageal cancer: validation and assessment of plan quality among different treatment centers. Radiat Oncol. 2015;10:220.
[12] Tol JP, Delaney AR, Dahele M, et al. Evaluation of a knowledge-based planning solution for head and neck cancer. Int J Radiat Oncol Biol Phys. 2015;91:612–620.
[13] Fogliata A, Belosi F, Clivio A, et al. On the pre-clinical validation of a commercial model-based optimisation engine: application to volumetric modulated arc therapy for patients with lung or prostate cancer. Radiother Oncol. 2014;113:385–391.

[14] Ong CL, Verbakel WFAR, Dahele M, et al. Fast arc delivery for stereotactic body radiotherapy of vertebral and lung tumors. Int J Radiat Oncol Biol Phys. 2012;83:e137–e143.
[15] Stephans KL, Djemil T, Tendulkar RD, et al. Prediction of chest wall toxicity from lung stereotactic body radiotherapy (SBRT). Int J Radiat Oncol Biol Phys. 2012;82:974–980.
[16] Ong CL, Palma D, Verbakel WFAR, et al. Treatment of large stage I–II lung tumors using stereotactic body radiotherapy (SBRT): Planning considerations and early toxicity. Radiother Oncol. 2010;97:431–436.
[17] Tol JP, Dahele M, Doornaert P, et al. Toward optimal organ at risk sparing in complex volumetric modulated arc therapy: an exponential trade-off with target volume dose homogeneity. Med Phys. 2014;41:021722.
[18] Ong CL, Verbakel WFAR, Cuijpers JP, et al. Stereotactic radiotherapy for peripheral lung tumors: a comparison of volumetric modulated arc therapy with 3 other delivery techniques. Radiother Oncol. 2010;97:437–442.
[19] Delaney AR, Tol JP, Dahele M, et al. Effect of dosimetric outliers on the performance of a commercial knowledge-based planning solution. Int J Radiat Oncol Biol Phys. 2016;94:469–477.

LETTER TO THE EDITOR

Adjuvant postoperative radiotherapy for cutaneous melanoma

William M. Mendenhall[a], Robert J. Amdur[a], Christopher G. Morris[a], Jessica Kirwan[a], Christiana Shaw[b] and Peter T. Dziegielewski[c]

[a]Departments of Radiation Oncology, University of Florida College of Medicine, Gainesville, FL, USA; [b]Departments of Surgery, University of Florida College of Medicine, Gainesville, FL, USA; [c]Departments of Otolaryngology, University of Florida College of Medicine, Gainesville, FL, USA

Introduction

Although surgery is the mainstay of treatment for patients with cutaneous melanoma, a subset of patients present with local–regionally advanced disease and are at high risk of a local–regional recurrence after surgery alone [1]. Postoperative radiotherapy (RT) has been shown to reduce the likelihood of local–regional recurrence and may be given with either a conventional fractionation schedule at 2 Gy per once daily fraction to doses ranging from 60 to 70 Gy or a hypofractionated schedule such as 30 Gy in 5 twice weekly fractions [2–4]. The latter schedule is likely more cost-effective and logistically more attractive for a group of patients at high risk of distant metastases who might benefit from adjuvant systemic therapy. The purpose of this paper is to update our experience with adjuvant postoperative RT for patients treated with curative intent for high-risk cutaneous melanoma [5,6].

Material and methods

Between August, 1981 and November 2014, 112 patients with cutaneous melanoma were treated with surgery and postoperative RT with curative intent. Eighty-one patients (72%) were male and 110 patients (98%) were Caucasian. The median age was 62 years (range, 21 to >89 years). The primary site was head and neck in 80 patients (71%) and elsewhere in the remainder. Patients had one or more of the following factors thought to be high risk after surgery alone: recurrence after prior surgery, positive lymph nodes, extracapsular extension, incomplete regional node dissection, incomplete or close (<5 mm) margins, gross residual disease and in-transit metastases. Sixty-three patients (56%) had cancers that were recurrent after prior surgery. Eighteen patients (16%) had in-transit metastases. Margins were negative in 84 patients (75%), close in one patient (1%), microscopically positive in 16 patients (14%), and gross residual disease was present in three patients (3%). Elective nodal RT was administered to eight patients (7%) who either had a clinically positive node excised or a positive sentinel lymph node biopsy without a completion dissection. The number of high-risk factors were: 1, 30 patients (27%); 2, 43 patients (38%); 3, 27 patients (24%); and 4 or more, 12 patients (11%).

Patients were treated with photons and/or electrons depending on the site and extent of the target volume. Intensity-modulated RT has been employed, when appropriate, since 2001. Eighty-four patients (75%) received 30 Gy in 5 twice-weekly fractions over 2.5 weeks; the remainder were treated with conventional fractionation at approximately 2 Gy per once daily fraction. Median follow-up times overall and for survivors were 2.8 years (range, 0.1 to 20.7 years) and 7.5 years (range, 0.9 to 20.7 years), respectively.

Statistical analyses were performed using SAS and JMP software (SAS Institute, Cary, NC). Time dependent outcomes including in-field local–regional control (LRC), overall LRC including out-of-field failures, distant metastasis-free survival, cause-specific survival, and overall survival were estimated using the Kaplan–Meier product limit method [7]. The level of statistical significance between strata of selected prognostic factors was tested with the log rank statistic.

CONTACT William M. Mendenhall mendwm@shands.ufl.edu Departments of Radiation Oncology, University of Florida College of Medicine, 2000 SW Archer Rd., PO Box 100385, Gainesville, Florida, USA

Supplemental data for this article can be accessed here.

http://dx.doi.org/10.1080/0284186X.2017.1295168